Kinetic Mechanism of Reaction between TT-Phase Niobium Oxide and Carbon Tetrachloride (CCl₄)

Kohki Ebitani, Yoshiaki Hirano, and Akira Morikawa[1]

Department of Chemical Engineering, Tokyo Institute of Technology, 2-12-1 Ookayama, Meguro-ku, Tokyo 152, Japan

The kinetic mechanism of reaction between TT-phase niobium oxide and carbon tetrachloride (CCl₄) at low (453 K) and high (above 573 K) temperatures was investigated. The reaction of the TT-phase niobium oxide with CCl₄ at 453 K was controlled by the diffusion of CCl₄ through the outer layer of the reaction product, NbOCl₃, formed around the surface. For the reaction at temperatures above 573 K, the chemical reaction on the surface of the niobium oxide controls the total reaction rate due to the disappearance of the layer of NbOCl₃. © 1995 Academic Press, Inc.

INTRODUCTION

The increasing importance of the decomposition of halogen-containing carbon compounds is due to their uses in the decomposition of chlorofluorocarbons (CFCs) into harmless compounds and in the halogenation of metal oxides, which is a valuable step in the metallurgy of refractory metals. The authors have investigated the decomposition of carbon tetrachloride (CCl₄) by the use of a metal oxide, as a model reaction of C–Cl bond cleavage, which has been proposed as an important step in the whole CFC decomposition (1, 2). In our previous work (3), niobium oxide in TT-phase was found to oxidize CCl₄ into CO₂ very selectively (without formation of COCl₂) at 453 K in the various metal oxides tested: amorphous Nb₂O₅, SiO₂–Al₂O₃, Al₂O₃, V₂O₅, TiO₂, and ZrO₂ in the absence of water and O₂. Since O₂ was not supplied as a reactant, the CCl₄ was oxidized into CO₂ by lattice oxygen atoms of the TT-phase niobium oxide. This reaction occurs at the gas–solid interface.

In this paper, the kinetic mechanism of the reaction between TT-phase niobium oxide and CCl₄, from the point of view of the oxidation of CCl₄ by the lattice oxygen of the TT-phase niobium oxide or the reduction of TT-phase niobium oxide by CCl₄, was determined from the dependence of the reaction rate on (a) the reaction time, reaction temperature, and pressure of CCl₄, and (b)

the geometry of the solid of the metal oxides and an analysis of the solid products. The experimental results led to the proposal that the diffusion-controlled mechanism and the chemical-reaction-controlled mechanism are dominant at reaction temperatures below 473 K and above 573 K, respectively.

EXPERIMENTAL

The TT-phase niobium oxide was prepared by calcination of niobic acid (Nb₂O₅ · nH₂O, No. AD-350 of Companhia Brasileira de Metalurgia e Mineracão (CBMM)) at 1023 K. The TT-phase of the niobium oxide was evidence by its X-ray diffraction pattern. The phase transformation from the amorphous phase to the TT phase of the niobium oxide at 1023 K was verified by observing the exothermic peak at around 840 K during the differential thermal analysis (DTA). The Nb content in the niobic acid was 55.7 wt%. The BET surface area of the metal oxide was determined by N₂ adsorption at 77 K.

The reaction of metal oxide (0.2 g) with CCl₄ was carried out under atmospheric pressure in a tubular flow reactor made of quartz with an inner diameter of 12.5 mm. A typical condition was CCl₄ 4.5 kPa, He 96.8 kPa, total flow rate 2.4 liter/hr, $W/F = 0.083$ g · hr · liter⁻¹. Unless otherwise stated, the metal oxide powder of 10–20 mesh was used after crushing the powder disk, which was formed under 200 kg/cm² pressure. The reaction temperature was monitored by a Chromel–Alumel thermocouple. The CCl₄ was supplied to the reaction passing a helium carrier through CCl₄ saturators and a column of MgSO₄ powder to dry the gas mixture. The partial pressure at CCl₄ was varied by changing the temperature of the CCl₄ saturators. Products (CO₂ and COCl₂) and the residual CCl₄ were analyzed by on-line gas-chromatography in a Gaskuropack-54 column. The outlet gas was passed through a K₂CO₃ aqueous solution (0.5 *M*), and trapped chlorides were quantified by AgNO₃ and Na₂S₂O₃ titration. In the absence of metal oxide in the quartz reactor, CCl₄ decomposition did not occur under the present experimental conditions.

The degree of reduction of the niobium oxide, α, CO_2 selectivity, Sel, and CCl_4 conversion were calculated by the following equations:

$$\alpha = \frac{\text{Number of oxygen atoms in the products } (CO_2, COCl_2) \text{ integrated over a certain process time}}{\text{Number of oxygen atoms in niobium oxide } (Nb_2O_5) \text{ packed into the reactor}}$$

$$Sel = \frac{\text{amount of } CO_2 \text{ formed}}{\text{amount of } CO_2 \text{ formed} + \text{amount of } COCl_2 \text{ formed}} \times 100 \ (\%), \text{ and}$$

$$CCl_4 \text{ conversion} = \frac{[CCl_4]\text{in} - [CCl_4]\text{out}}{[CCl_4]\text{in}} \times 100 \ (\%).$$

In order to evaluate the distribution of the chlorine along the depth from the surface in the niobium oxide after the reaction with CCl_4, the energy dispersed X-ray spectroscopic (EDS) measurements were conducted on an EDAX PV9900I (Phillips Co., Ltd.).

RESULTS AND DISCUSSION

As reported previously (3), Nb_2O_5 exhibited a higher activity at 453 K than any other metal oxide. In addition, Nb_2O_5 treated at 1023 K (TT-phase niobium oxide) shows much higher selectivity for CO_2 (100%) at 453 K than that treated at 573 K (amorphous niobium oxide). The BET surface area of the Nb_2O_5 degassed at 573 K was 120 m^2/g, which decreased to 50 m^2/g for Nb_2O_5 degassed at 873 K. Thus, the specific activity (per surface area) for CO_2 formation of the Nb_2O_5 treated at 1023 K (TT-phase niobium oxide) is four times greater than that of the Nb_2O_5 treated at 573 K (amorphous niobium oxide). The carbon balance on the TT-phase niobium oxide at the process time of 3 hr at 453 K was ca. 95%, indicating that carbon compounds did not remain on the surface during the reaction.

Figure 1 shows the change with increasing process time in the CCl_4 conversion (left axis) and CO_2 selectivity (right axis) of the TT-phase niobium oxide at various reaction temperatures (453–723 K). At any reaction temperature, the CCl_4 conversion gradually decreased as the process time increased. At reaction temperatures higher than 673 K, the CCl_4 conversion decreased to almost zero and the reactant Nb_2O_5 disappeared after several hours, indicating a complete reaction of TT-phase niobium oxide with CCl_4. The products were CO_2 and $COCl_2$ (phosgene). No carbon monoxide (CO) was detected at any reaction temperature or at any process time. The CO_2 selectivity for the reaction at 453 K was extremely high compared to that at other reaction temperatures. Since O_2 was not supplied as a reactant, the CCl_4 was oxidized

into CO_2 or $COCl_2$ only by lattice oxygen atoms of the TT-phase niobium oxide.

The change in α (degree of reduction of TT-phase niobium oxide) as a function of the process time at various reaction temperatures (573–773 K) is shown in Fig. 2. At higher reaction temperatures (723 and 773 K), the value of α becomes a constant value of 0.6 for longer process times. The value of 0.6 means that 60% of the oxygen of the TT-phase niobium oxide was removed by the reaction with CCl_4. After the reaction at 723 and 773 K, the solid did not remain on the reactor bed; a white powder with a yellowish cast was deposited at the outlet of the reactor. The powder was dissolved in deionized water without exposure to air and the amount of Cl^- ion in the solution (pH < 7) was determined by titration using Mohr's method. The ratios of the amount of Cl^- in the solution to the amount of niobium in the powders obtained from the reaction at 623 and 723 K were 3.03 and 2.98, respectively. This ratio of $Cl/Nb = 3.0$ corresponds to $NbOCl_3$, which is white. The yellowish cast in the powder may be due to a small amount of $NbCl_5$, which is yellow.

The following two reactions are used to explain the experimental results:

$$Nb_2O_5 + 2CCl_4 \rightarrow 2NbOCl_3 + CO_2 + COCl_2 \quad [1]$$

$$2Nb_2O_5 + 3CCl_4 \rightarrow 4NbOCl_3 + 3CO_2. \quad [2]$$

Equation [2] is obtained by taking into account the further reaction of $COCl_2$ with Nb_2O_5. Both of these reactions occur in the present reaction system; the value of α at the completion of the reaction is 0.6, which corresponds well to the experimental results (Fig. 2).

When the overall reaction in the present system is mainly controlled by Eq. [1], the selectivity of CO_2 is 50%. While the system is adequate to achieve the full oxidation of CCl_4 to give CO_2, as indicated by Eq. [2], in such a case, as the system retains a sufficient amount of oxidant, Nb_2O_5, and because of the low temperature of the reaction, the selectivity must be close to 100%. The latter case corresponds to the result shown in Fig. 1a, and the results of Figs. 1b–1e are mainly explained by Eq. [1].

In order to estimate a precise reaction rate, the CCl_4 conversion and CO_2 selectivity were compared at the same α value (the degree of reduction of the niobium oxide). The changes in the reaction rate and CO_2 selectivity as a function of the reaction temperature at constant α of 0.2 are shown in Fig. 3. The total reaction rate, or the sum of the formation rates of CO_2 and $COCl_2$, increased as the reaction temperature increased. The increase in the rate of $COCl_2$ formation is not remarkable, while that of CO_2 is dramatic. This was demonstrated well by the change in CO_2 selectivity with reaction temperature.
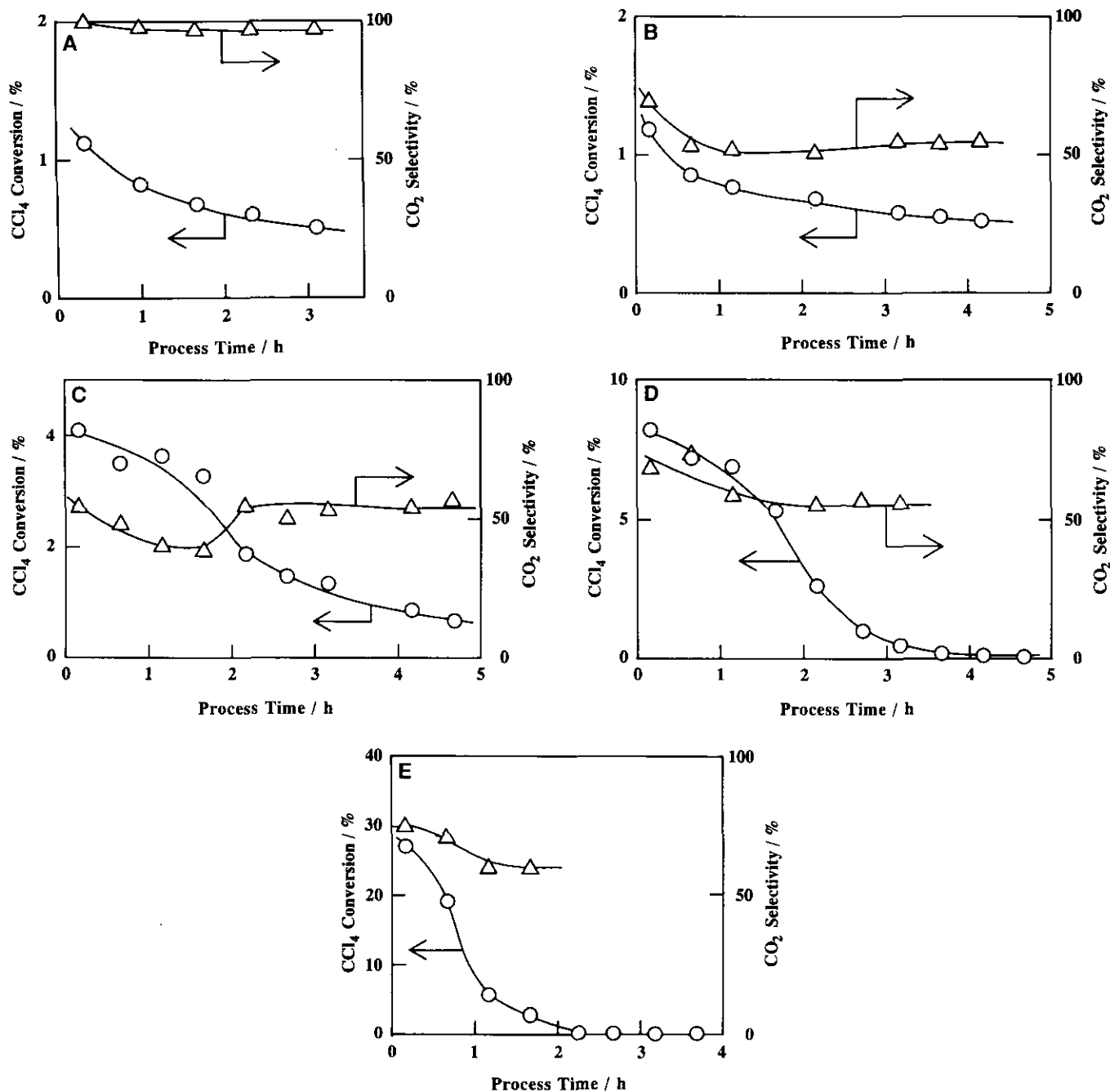
FIG. 1. The time course of CCl₄ conversion (left axis) and CO₂ selectivity (right axis) on TT-phase niobium oxide at (A) 453, (B) 573, (C) 623, (D) 673, and (E) 723 K.

Figure 4 shows a plot of the logarithm of the (total) reaction rate to a reciprocal of the reaction temperature at a constant α of 0.2. The apparent activation energies for CO_2 and $COCl_2$ formations were 96.6 kJ mole⁻¹ (23.8 kcal mole⁻¹) and 54.2 kJ mole⁻¹ (13.0 kcal mole⁻¹), respectively. These values were almost unchanged at various values of α: 0.1 or 0.3. This apparent activation energy was smaller that that obtained by Mehra *et al.* for

the chlorination of Nb_2O_5 by chlorine in the presence of excess graphite (4). A very low activation energy for the rate of $COCl_2$ formation may be observed due to the fact that $COCl_2$ is an intermediate in the reaction to give a complete oxidation product, CO_2(3).

Figure 5 shows a plot of the logarithm of the formation rate of CO_2 to the logarithm of CCl_4 pressure at a constant α of 0.05 at 453 K. The rate of CO_2 formation de-
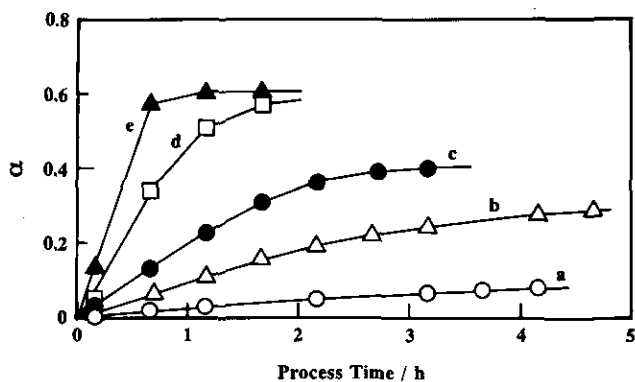
FIG. 2. The changes in α (degree of reduction of TT-phase niobium oxide) as a function of time at (a) 573, (b) 623, (c) 673, (d) 723, and (e) 773 K.

creased as the CCl_4 pressure increased. Apparently, the reaction order is negative with respect to the CCl_4 pressure at 453 K.

A plot of the logarithm of the formation rates of CO_2 (a) and of $COCl_2$ (b) to the logarithm of CCl_4 pressure at a constant α of 0.20 at 623 K is shown in Fig. 6. The rates of CO_2 and $COCl_2$ formation increased as the CCl_4 pres-
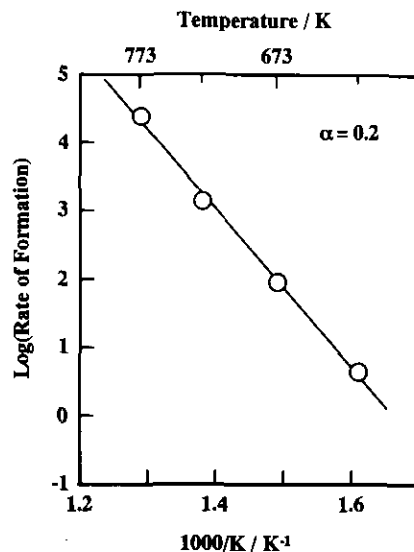

FIG. 4. Plot of the logarithm of the reaction rate and a reciprocal of the reaction temperature for the reaction of CCl_4 and the TT-phase niobium oxide at α of 0.2.

sure increased. The difference in the dependence of the reaction rate on the CCl_4 pressure between the reaction at 453 and at 623 K may be related to the different reaction features.

Generally, the reduction of the metal oxide, assuming a contracting sphere model, is expressed as

$$\frac{k_p}{r_0 d_0}(C_0 - C_{eq})t = [1 - (1 - \alpha)^{1/3}]$$

$$+ \frac{r_0 k_p}{k_d}[1/2 - \alpha/3 - (1 - \alpha)^{2/3}], \quad [3]$$

FIG. 3. The changes in the reaction rate and CO_2 selectivity for the reaction of CCl_4 and TT-phase niobium oxide as a function of the reaction temperature at a constant α ($\alpha = 0.2$).
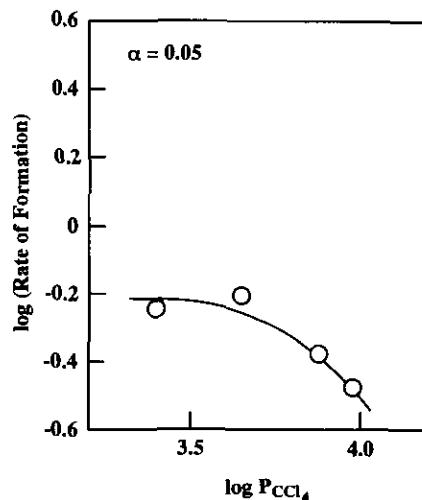

FIG. 5. Plot of the logarithm of the reaction rate and logarithm of CCl_4 pressure for the reaction of CCl_4 and the TT-phase niobium oxide at a constant α ($\alpha = 0.05$) at 453 K.
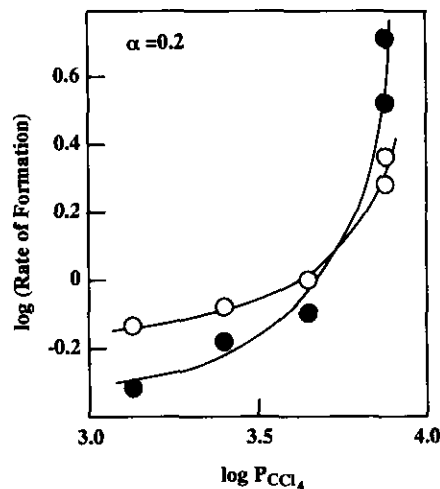
FIG. 6. Plot of the Logarithm of the reaction rates for (a) CO_2 and (b) $COCl_2$ and logarithm of CCl_4 pressure for the reaction of CCl_4 and the TT-phase niobium oxide at a constant α ($\alpha = 0.20$) at 623 K.

where α is the degree of reduction, r_0 is the radius of metal oxide at initiation, C_0 is the concentration of CCl_4 at r_0, C_{eq} is the equilibrium concentration of CCl_4, d_0 is the density at r_0, k_p is the rate constant of the CCl_4 reaction, and k_d is the diffusion coefficient of CCl_4 (5). This is the integrated rate equation giving the degree of reduction, α, as a function of time t.

If $k_p \ll k_d$ or $k_p/k_d \doteq 0$, then

$$\frac{k_p}{r_0 d_0}(C_0 - C_{eq})t = [1 - (1 - \alpha)^{1/3}]. \qquad [4]$$

If $k_p \gg k_d$ or $k_d/k_p \doteq 0$, then

$$\frac{k_p}{r_0 d_0}(C_0 - C_{eq})t = \frac{r_0 k_p}{k_d}[1/2 - \alpha/e - (1 - \alpha)^{2/3}/2]. \qquad [5]$$

A linear correlation between $[1 - (1 - \alpha)^{1/3}]$ and t indicates chemical reaction control at the metal oxide/reduced phase interface. If the overall reaction rate is limited by the diffusion of reductant (CCl_4, in this case) through the reaction product layer, a plot of $[1/2 - \alpha/3 - (1 - \alpha)^{2/3}/2]$ against t may be a straight line.

Figure 7 shows a plot of $[1/2 - \alpha/3 - (1 - \alpha)^{2/3}/2]$ against the process time, t, for the reaction at 453 K. A plot of $[1 - (1 - \alpha)^{1/3}]$ against t for the same reaction is shown in Fig. 8. As seen from these figures, the plot in Fig. 7, rather than that in Fig. 8, fits a straight line, suggesting that the diffusion control mechanism is dominant for the reaction at 453 K. It is plausible that the CCl_4 diffuses slowly through the product layer formed on the surface of the niobium oxide and reacts rapidly with niobium oxide at the interface between the niobium oxide
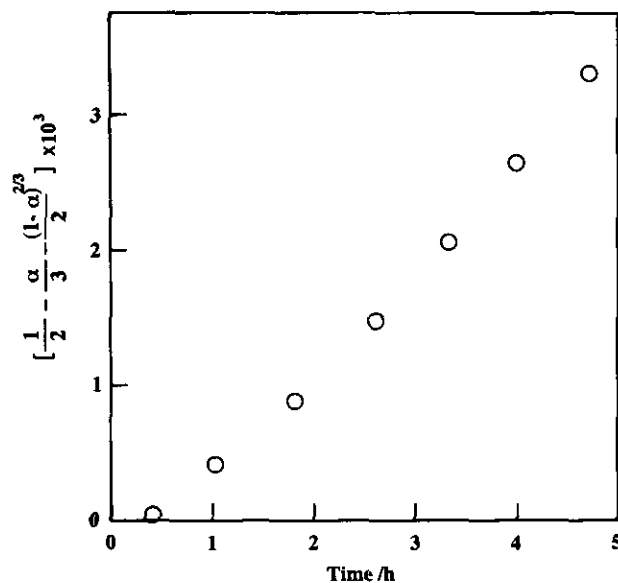

FIG. 7. Plot of $[1/2 - \alpha/3 - (1 - \alpha)^{2/3}/2]$ versus time for the reaction of TT-phase niobium oxide with CCl_4 at 453 K.

and the product layer. The temperature of 453 K is rather low for the product, $NbOCl_3$, to be subsumed, and the reacting surface of the niobium oxide must be covered by a layer of the product, $NbOCl_3$. The vapor pressure of $NbOCl_3$ at 600 K is about 1 atm (6).

Figure 9 shows the relationship between the rate of CO_2 formation per gram or per apparent outer area of the pellet after the process time of 1 hr and the amount of TT-phase niobium oxide at 453 K. As clearly shown, the rate per apparent surface area of the pellet was constant for different sizes of niobium oxide pellets, whereas the rate per gram of the pellet was not. This strongly indicates that the reaction of the TT-phase niobium oxide with CCl_4 at 453 K was controlled by the diffusion of the CCl_4
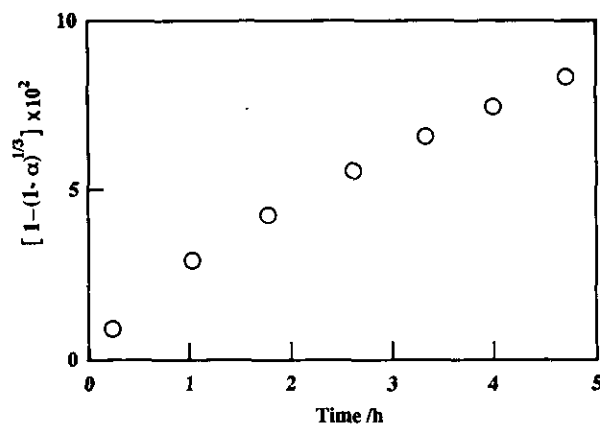

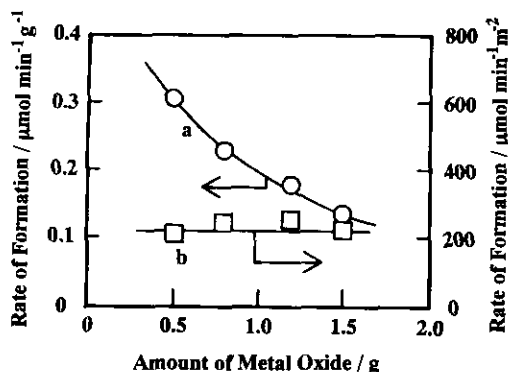FIG. 8. Plot of $[1 - (1 - \alpha)^{1/3}]$ versus time for the reaction of TT-phase niobium oxide with CCl_4 at 453 K.

FIG. 9. Relationship between the rate of formation (per gram and per apparent area) and the amount of TT-phase niobium oxide at 453 K.

FIG. 11. Plot of $[1 - (1 - \alpha)^{1/3}]$ versus time for the reaction of TT-phase niobium oxide with CCl_4 at 573 (a), 623 (b), and 673 K (c).

through the outer layer of the oxide pellet, and that the inner niobium oxide did not encounter the reactant CCl_4. The EDS profile of the pellet after the reaction of CCl_4 ($\alpha = 0.012$ for 5 hr for the TT-phase niobium oxide) revealed that the Cl element was detected only near the outer surface of the oxide pellet.

The reaction mechanism of the TT-phase niobium oxide with CCl_4 at reaction temperatures higher than 573 K seems to be different from that operating in the reaction at 453 K. Figure 10 shows the plots of $[1/2 - \alpha/3 - (1 - \alpha)^{2/3}/2]$ versus time for the reaction of TT-phase niobium oxide with CCl_4 at 573 K (a), 623 (K (b), and 673 K (c). The plots of $[1 - (1 - \alpha)^{1/3}]$ versus time for the reaction of TT-phase niobium oxide with CCl_4 at 573 K (a), 623 K
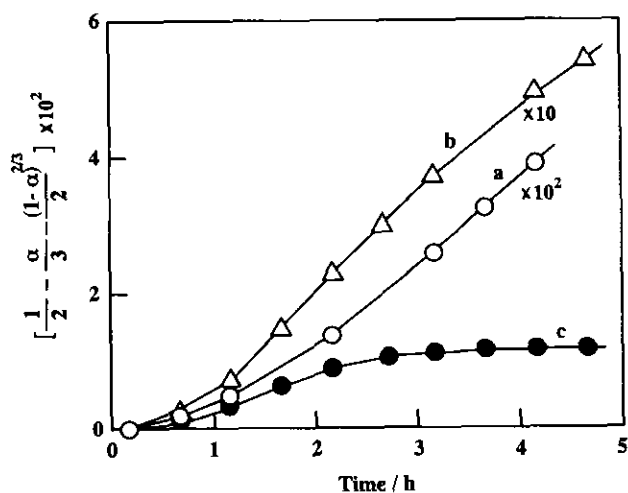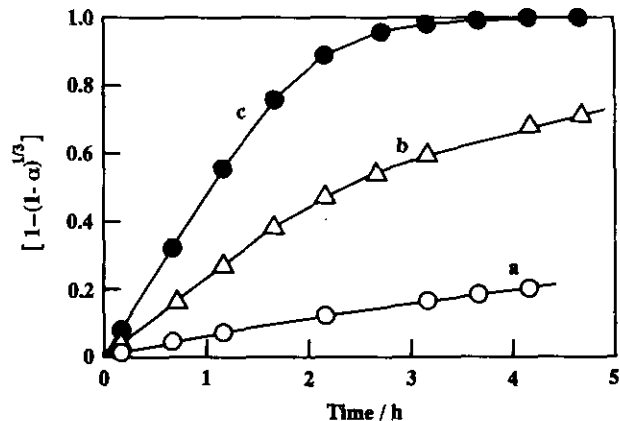

FIG. 10. Plot of $[1/2 - \alpha/3 - (1 - \alpha)^{2/3}/2]$ versus time for the reaction of TT-phase niobium oxide with CCl_4 at 573 (a), 623 (b) and 673 K (c).

(b), and 673 K (c) are shown in Fig. 11. It seems that the plots of $[1 - (1 - \alpha)^{1/3}$ versus time within 2 or 3 hr were straight; the plots of $[1/2 - \alpha/3 - (1 - \alpha)^{2/3}/2]$ versus time were not. This suggests that a chemical reaction control mechanism was dominant at reaction temperatures above 573 K. In this situation, the outer layer around the unreacted niobium oxide was removed to the vapor phase: the diffusion of CCl_4 through the outer layer could not be considered.

The extremely high CO_2 selectivity (deep oxidation of CCl_4) observed at the reaction temperature of 453 K might be caused by a long contact time at the unreacted niobium oxide/$NbOCl_3$ interface, since the CCl_4 concentration at the interface is apparently very small. Even though $COCl_2$ is formed on the reacting surface, it must be oxidized by oxygenates released from the bulk of the oxide. The strong positive dependence of the reaction rate on the CCl_4 pressure observed for the reaction at 623 K might be caused by an increase in adsorbed CCl_4 on the TT-phase niobium oxide surface through chemical interaction increasing the CCl_4 pressure.

The reaction control mechanism was different for the reactions at temperatures lower than 500 K and those at temperatures higher than 550 K. The vapor pressure of the $NbOCl_3$, which is considered to form the outer layer on the unreacted niobium oxide surface, exceeds 760 mmHg at around 600 K. Thus, at the lower temperature, the reaction is controlled by the diffusion of the reacting gas through the product layer formed around the niobium oxide surface.

In conclusion, the reaction of the TT-phase niobium oxide with CCl_4 at 453 K was controlled by the diffusion of CCl_4 through the outer layer of reaction product, $NbOCl_3$, formed around the outer layer of reaction product, $NbOCl_3$, formed around the niobium oxide surface.

For the reaction at temperatures above 573 K, the chemical reaction occurring on the surface of the niobium oxide controls the total reaction rate, due to the disappearance of the layer of $NbOCl_3$ by its sublimation.

ACKNOWLEDGMENTS

REFERENCES

1. S. Okazaki and A. Kurosaki, *Chem. Lett.*, 1901 (1989).
2. K. Mizuno, Meeting abstracts of "International Forum on Environmental Catalysis—1993," p. 29. Tokyo, Japan, 1993.
3. K. Ebitani, Y. Hirano, J.-H. Kim, and A. Morikawa, *React. Kinet. Catal. Lett.* **51,** 351 (1993).
4. O. K. Mehra, S. Zahed Hussain, and P. K. Jena, *Trans. Indian Inst. Met.* **19,** 53 (1966).
5. N. W. Hurst, S. J. Gentry, A. Jones, and B. D. McNicol, *Catal. Rev.-Sci. Eng.* **24,** 233 (1982).
6. F. Fairbrother, "The Chemistry of Niobium and Tantalum," Chap. 4, Elsevier, Amsterdam, 1967.